Geochemistry International, Vol. 42, No. 2, 2004, pp. 97–105. Translated from Geokhimiya, No. 2, 2004, pp. 131–141.

Timing of Syenite Intrusions on the Eastern Slope of the Sredinnyi Range, Kamchatka: Rate of Accretionary Structure Exhumation

J. K. Hourigan*, A. V. Solov'ev, G. V. Ledneva**, J. I. Garver***, M. T. Brandon*, and P. W. Reiners***

** Department of Geology and Geophysics, Yale University, P.O. Box 208109, New Haven, CT 06520-8109, United States*

*** Institute of the Lithosphere of Marginal Seas, Russian Academy of Sciences, Staromonetnyi per. 22, Moscow, 109180 Russia*

e-mail: solov@ilran.ru

**** Department of Geology, Union College, Union Ave. 807, Schenektady, NY 12308-2311, United States*

Received March 13, 2002

Abstract—The isotopic thermochronological study included the U–Pb (SHRIMP) and fission-track dating of zircon and fission-track and (U–Th)–He dating of apatite from syenite intrusions cropping out in the eastern slope of the Sredinnyi Range of Kamchatka. The emplacement time of the intrusion was determined, and its exhumation velocity was evaluated. According to U–Pb (SHRIMP) zircon dating, the age of syenite crystallization (63.0 ± 0.6 and 70.4 ± 0.7 Ma) corresponds to the Late Cretaceous and Early Paleogene. Starting from 25 Ma, the cooling rate of the intrusion, which was likely controlled by exhumation, varied from 4 °C/Ma to 20 °C/Ma. If the geothermal gradient is assumed to be 30 °C/km, the exhumation rate of the intrusion from the Late Oligocene and until now ranged from 0.18 km/Ma to 0.67 km/Ma.

INTRODUCTION

The quantitative estimation of the exhumation rates of rock complexes in convergent margins is one of the most important problems of modern geodynamics. This estimation was made possible by achievements in the development of new high–precision timing methods that can be applied to various minerals, as well as thanks to recent data on the closure temperatures of isotopic systems in minerals. Thermochronology is a method aimed at reconstructing the thermal history of geological complexes based on their apparent isotopic ages and is widely applied to dating tectonic processes. Unfortunately, the studies in this field in Russia remain scanty, first of all, because of the lack of required state-of-the art equipment. We have carried out U–Pb (SHRIMP) and fission-track dating of zircon and fission-track and (U–Th)–He dating of apatite from syenite intrusions exposed in the eastern slope of the Sredinnyi Range in Kamchatka. This allowed us to date intrusion crystallization and to estimate quantitatively the exhumation rate of the rocksits. Our research demonstrates, using the example of the syenite massifs, the methodical aspects of studying rock exhumation in convergent margins.

GEOLOGICAL SETTING OF THE SYENITE INTRUSIONS IN THE SREDINNYI RANGE OF KAMCHATKA

The three pre-Cenozoic structural complexes recognized in the eastern slope of the Sredinnyi Range of Kamchatka are (from bottom to top): (1) rocks of the high-grade metamorphic core (Kolpakovo Complex), (2) rocks of the metamorphic cover (Malka Complex, including the Shikhtinskaya, Andrianovskaya, Kheivanskaya, and Khimkinskaya formations), and (3) unmetamorphosed volcanic and sedimentary rocks of the Cretaceous island-arc system (Irunei and Kirganik formations). The Shikhtinskaya Formation (Kamchatka Group) of metaterrigenous rocks is overthrust by metavolcanic rocks of the Andrianovskaya Formation [1]. The Late Cretaceous island-arc complexes (Irunei and Kirganik Formations) are, in turn, thrust over the rocks of Andrianovskaya Formation. The multiphase dunite–clinopyroxenite and clinopyroxenite–gabbro massifs, e.g., the Levoandrianovskii massif (Fig. 1) are often regarded as fragments of conduits related to the island-arc volcanics [2].

Syenite intrusions in the eastern slope of the Sredinnyi Range of Kamchatka cut the tuffaceous–terrigenous and volcanogenic terrigenous rocks of the Andrianovskaya Formation (island-arc complexes of uncertain age), which were metamorphosed to the green-

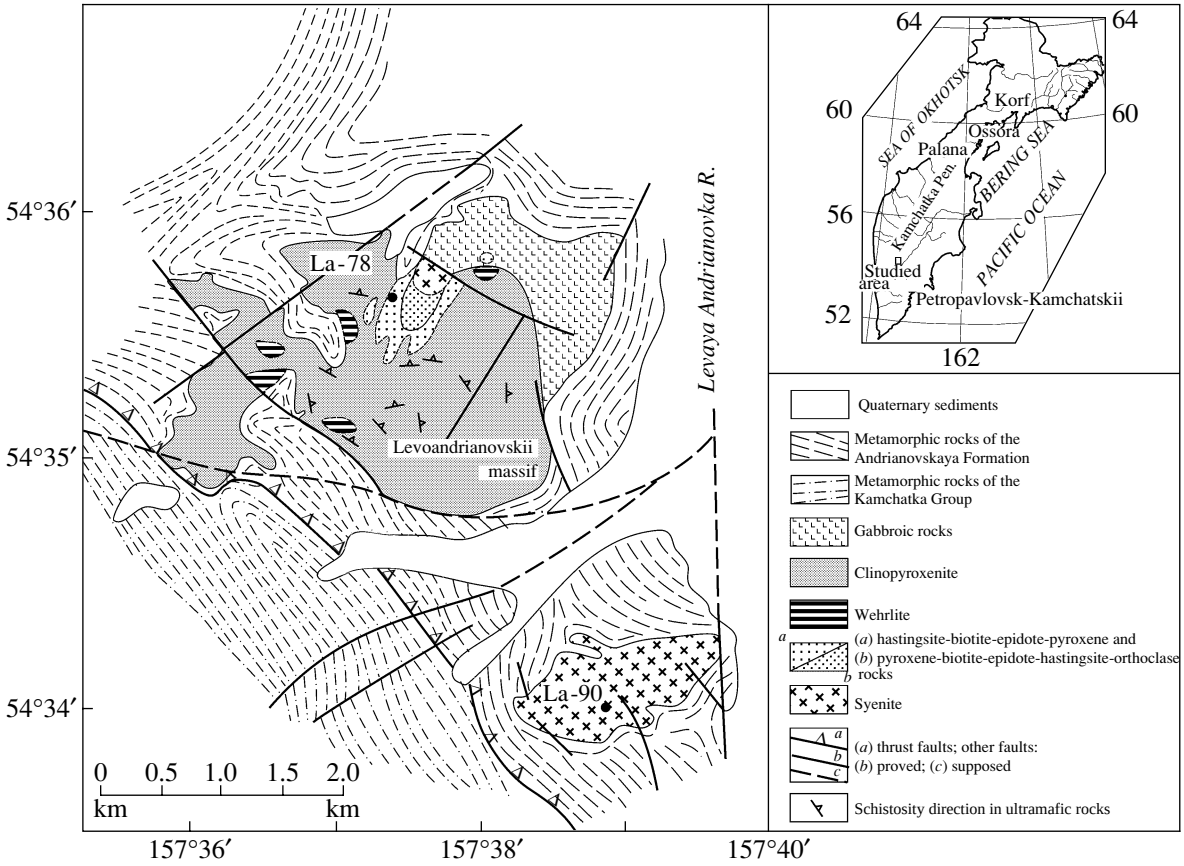

Fig. 1. Schematic geological map of the Levoandrianovskii massif and syenite intrusions in the eastern slope of the Sredinnyi Range of Kamchatka, after [2] and data reported by M.N. Shapiro.

schist and amphibolite facies, as well as multiphase dunite–clinopyroxenite and clinopyroxenite–gabbro massifs [2]. The marginal zones of the syenite intrusions are foliated (M.N. Shapiro, personal communication), and this suggests that they had been intruded before the metamorphic overprint on the rocks of Andianovskaya Formation. The metamorphosed island-arc rocks (Andrianovskaya Formation) make up a series of allochthonous tectonic slabs thrust over gneisses of the Kamchatka Group [1]. The Lower Eocene sediments deposited in the marginal continental environment served as the protolith of the gneisses [3].

Our samples were taken from two syenite intrusions in the middle and upper reaches of the Levaya Andrianovka River (Fig. 1). Sample LA-90 was taken from altered syenite that intrudes the tuffaceous–terrigenous rocks of the Andrianovskaya Formation, metamorphosed to the amphibolite facies, and Sample LA-78 is from a syenite intrusion in clinopyroxenite of the Levoandrianovskii massif (Fig. 1). Sample LA-90 is a hastingsite–pyroxene–orthoclase rock with a trachytoid texture. The origin of this rock is attributed to the autometasomatic alteration of amphibole syenite at 500–550°C [2]. Sample LA-78 is a hastingsite–biotite–epidote–albite–pyroxene–K-feldspar rock, which was formed as a result of interaction between the alkali syenite melt and the host clinopyroxenite [2].

THERMOCHRONOLOGY

Progress in isotopic geochronological methods led to the need of distinguishing between true and apparent ages and of introducing the concept of the closure temperature of an isotopic system [4].[1] The true age of a rock or mineral corresponds to the interval between the time of its formation and the present time. The time of crystallization is understood as the time of igneous rock formation, whereas the time of sedimentation or lithification is referred to as the time of sedimentary rock formation. When metamorphic rocks are studied, their protolith and metamorphism ages should be distinguished. The apparent age is the age of a rock (mineral) obtained by any isotopic method and differing from the true age. The temperature of isotopic system closure (blocking) is the temperature at which the rate of an isotope loss via diffusion becomes insignificant in com-

[1] These concepts and related topics are discussed in hundreds of publications. We quote here only one modern work intended for a wide circle of specialists.

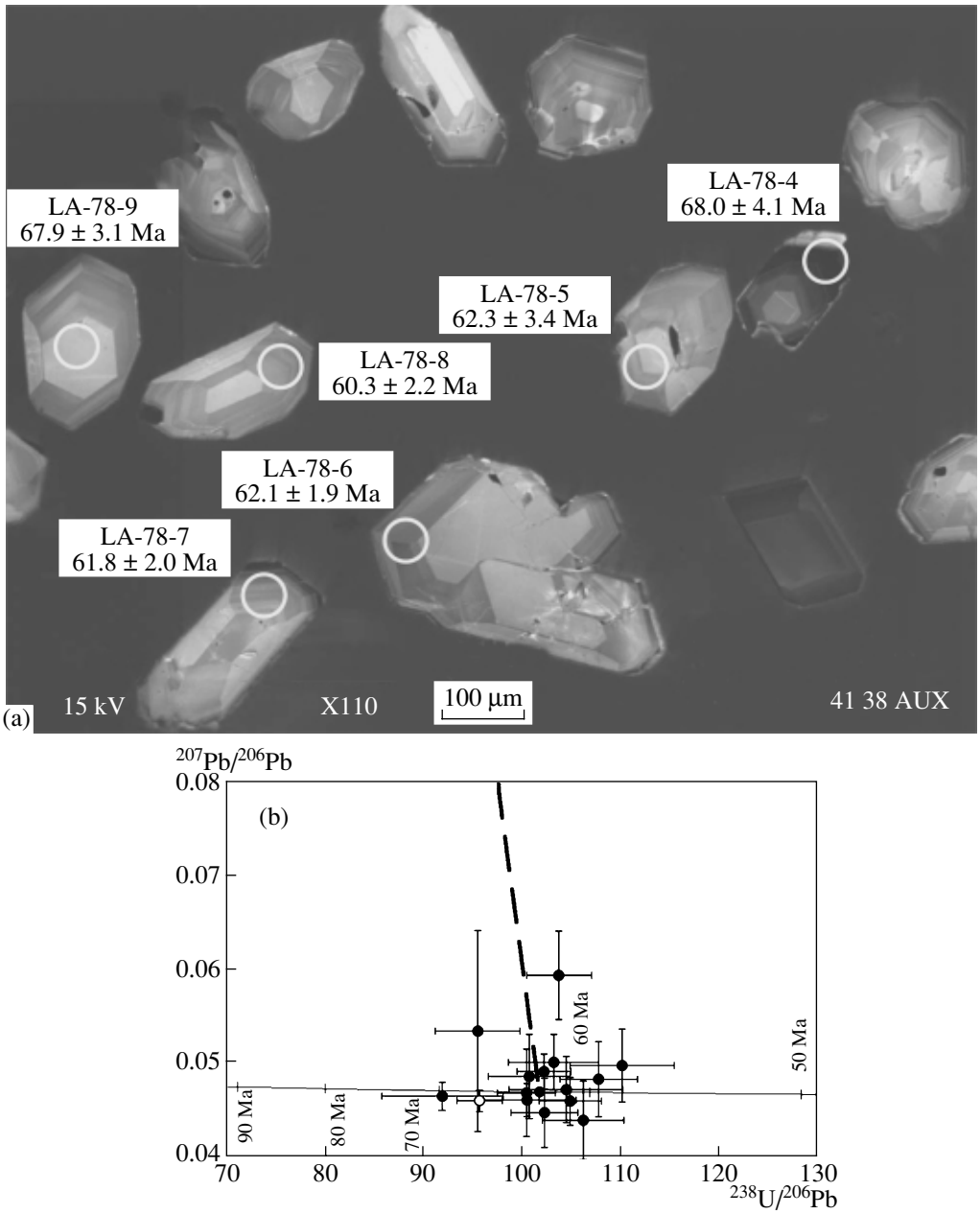

Fig. 2. (a) Cathode-luminescent images of zircon crystals from Sample LA-78 with dated grain numbers. The analyzed points are shown as white circles; age, Ma (±1σ) is also shown. (b) Tera–Wasserburg graph for Sample LA-78. The horizontal solid line is concordia. The dashed line is the mixing line of radiogenic lead (calculated as a weighed value of ^{207}Pb-corrected $^{206}Pb/^{238}U$ ages) and model common lead [12]. Uncorrected isotope ratios are shown with uncertainty ±1σ.

parison with isotope gain [5]. The measured apparent age is the time span from the moment when the mineral under study cooled to the temperature below its isotopic system closure. Various isotopic systems in various minerals have different closure temperatures [4–7]. Thus, dating different minerals from one rock by different geochronological methods offers an opportunity to determine its cooling (thermotectonic) record.

In this work, we dated zircon with U–Pb (SHRIMP) and fission-track methods and apatite with fission-track and (U–Th)–He methods. The minerals were picked out from two syenite samples (LA-78 and LA-90, see Fig. 1) at the Institute of the Lithosphere of Marginal Seas, Russian Academy of Sciences, using conventional techniques.

U–Pb (SHRIMP) Dating of Zircon

The temperature of the U–Pb system closure in zircon is above >900°C [8]. It is deemed that the age of magmatic zircon measured by the U–Pb method determines the time

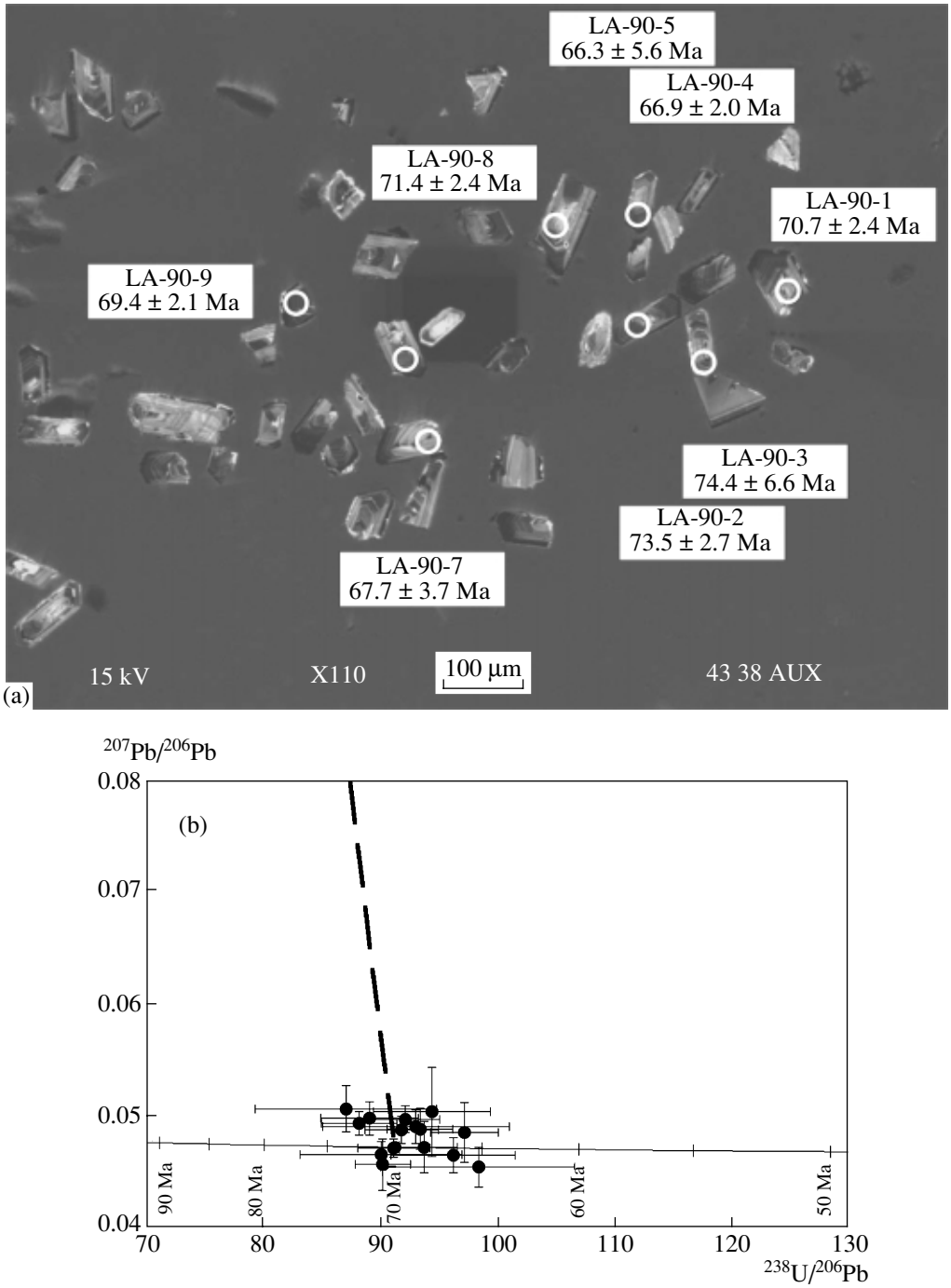

Fig. 3. (a) Cathode-luminescent images of zircon crystals from Sample LA-90 with dated grain numbers. The analyzed points are selected by white circles; age, Ma (±1σ) is also shown. (b) Tera–Wasserburg graph for Sample LA-90. The horizontal solid line is concordia. The dashed line is the mixing line of radiogenic lead (calculated as a weighed value of ^{207}Pb-corrected $^{206}Pb/^{238}U$ ages) and model common lead [12]. Uncorrected isotope ratios are shown with uncertainty ±1σ.

of intrusive rock emplacement and that the U–Pb system is not very susceptible to the thermal impacts.

About 50 zircon grains were picked out from each sample. Zircons from the samples and zircons of the AS57 standard [9] were placed into epoxy resin and polished. The zircon grains were checked in reflected and transmitted light at a magnification of 20× for the fractures and inclusions. A cathode-luminescence detector mounted on a JEOL JSM 5600 SEM was used to examine the zoning and internal structure of the polished zircon grains (Figs. 2, 3).

The isotopic measurements were carried out on a SHRIMP-RG (Sensitive High Resolution Ion Micro-Probe—Reverse Geometry) at Microanalytical USGS Center in Stanford following standard methods [10]. A beam of negatively charged oxygen ions was used to

Table 1. U–Pb age of individual zircon grains from syenite intrusions of the Sredinnyi Range, Kamchatka

Sample LA-78 (Figs. 1, 2)

Grain number	U, ppm	Th, ppm	Th/U	$^{207}Pb/^{206}Pb$	$^{238}U/^{206}Pb$	Age, Ma (σ)*
La-78-1	1703	1945	1.14	0.0468 ± 0.0015	91.98 ± 6.16	70.8 ± 4.7
La-78-2	438	184	0.42	0.0504 ± 0.0030	103.28 ± 4.59	62.8 ± 2.8
La-78-3	1046	973	0.93	0.0494 ± 0.0019	102.28 ± 2.72	63.5 ± 1.7
La-78-4	4566	3260	0.71	0.0464 ± 0.0011	95.74 ± 2.30	68.0 ± 1.6
La-78-5	303	184	0.61	0.0475 ± 0.0035	104.53 ± 5.78	62.2 ± 3.4
La-78-6	620	457	0.74	0.0463 ± 0.0025	104.96 ± 3.16	62.1 ± 1.9
La-78-7	283	105	0.37	0.0597 ± 0.0047	103.82 ± 3.29	61.8 ± 2.0
La-78-8	238	108	0.45	0.0486 ± 0.0040	107.85 ± 3.96	60.3 ± 2.2
La-78-9	95	37	0.38	0.0538 ± 0.0107	95.54 ± 4.29	67.6 ± 3.1
La-78-10	242	152	0.63	0.0472 ± 0.0047	100.49 ± 2.95	64.8 ± 1.9
La-78-11	426	215	0.50	0.0451 ± 0.0037	102.33 ± 3.38	63.8 ± 2.1
La-78-12	256	154	0.60	0.0489 ± 0.0045	100.81 ± 4.16	64.4 ± 2.7
La-78-13	397	181	0.46	0.0501 ± 0.0039	110.23 ± 5.30	58.9 ± 2.8
La-78-14	1417	957	0.68	0.0464 ± 0.0018	100.56 ± 4.99	64.8 ± 3.2
La-78-15	197	75	0.38	0.0443 ± 0.0042	106.27 ± 4.13	61.5 ± 2.4
Average age is 63.0 ± 0.6 Ma; MSWD = 0.86; *n* = 14 (except grain LA-78-4)						

Sample LA-90 (Figs. 1, 3)

Grain number	U, ppm	Th, ppm	Th/U	$^{207}Pb/^{206}Pb$	$^{238}U/^{206}Pb$	Age, Ma (σ)*
La-90-1	2010	967	0.48	0.0490 ± 0.0012	91.81 ± 3.12	70.7 ± 2.4
La-90-2	2543	1175	0.46	0.0496 ± 0.0010	88.20 ± 3.21	73.5 ± 2.7
La-90-3	1300	711	0.55	0.0508 ± 0.0021	87.04 ± 7.75	74.4 ± 6.6
La-90-4	616	177	0.29	0.0487 ± 0.0027	97.16 ± 2.88	66.9 ± 2.0
La-90-5	1166	315	0.27	0.0456 ± 0.0018	98.37 ± 8.36	66.3 ± 5.6
La-90-6	722	180	0.25	0.0459 ± 0.0023	90.20 ± 2.37	72.2 ± 1.9
La-90-7	1640	537	0.33	0.0467 ± 0.0016	96.20 ± 5.29	67.7 ± 3.7
La-90-8	3533	1597	0.45	0.0473 ± 0.0008	91.14 ± 3.08	71.4 ± 2.4
La-90-9	702	117	0.17	0.0474 ± 0.0023	93.74 ± 2.81	69.4 ± 2.1
La-90-10	1750	1111	0.63	0.0500 ± 0.0015	89.08 ± 4.17	72.8 ± 3.4
La-90-11	642	182	0.28	0.0506 ± 0.0040	94.40 ± 5.01	68.6 ± 3.6
La-90-12	2939	1001	0.34	0.0499 ± 0.0012	92.13 ± 2.95	70.4 ± 2.3
La-90-13	1499	798	0.53	0.0493 ± 0.0015	93.03 ± 7.96	69.8 ± 5.9
La-90-14	2459	2862	1.16	0.0468 ± 0.0012	90.04 ± 6.90	72.3 ± 5.5
La-90-15	1075	648	0.60	0.0491 ± 0.0018	93.37 ± 2.81	69.5 ± 2.1
Average age is 70.4 ± 0.7 Ma; MSWD = 0.60; *n* = 15						

* Age of individual grains calculated as a mean weighed ^{207}Pb value corrected by $^{206}Pb/^{238}U$ ages.

sputter positive ions from a ~30 μm diameter spot within the target crystal. Each measurement involved five cycles through the mass stations. The AS57 age standard was measured after every four or five measurements of the crystals with unknown age. The U and Th contents were calibrated against SL13 [11].

The ^{207}Pb correction applied to the ages presented in Table 1 is based on the assumption that slightly discordant zircons contain a simple mixture of common and radiogenic lead. The measured $^{207}Pb/^{206}Pb$ ratio is used for the common lead correction. The age was calculated by extrapolating the measured data over the concordia along the line corresponding to the model age of common lead [12] at an approximation for the age of single grains. The cathode-luminescence images indicate that the zircon grains do not contain xenocryst cores (Figs. 2a, 3a).

The zircons of Sample LA-78 are large (~200–400 μm) euhedral zonal crystals (Fig. 2a). The age calculated as a mean weighed ^{207}Pb value and corrected using the $^{206}Pb/^{238}U$ ages of 14 dated grains is 63.0 ± 0.6 Ma (±1σ); MSWD = 0.86 (Fig. 2b). The low MSWD indicates that the data scatter is related to analytical uncertainties. The age of grain LA-78-4, which was enriched in U and Th (Table 1), was rejected.

The zircons of Sample LA-90 are small (~100 μm) euhedral and subhedral zonal crystals (Fig. 3a). The age calculated as a mean weighed ^{207}Pb value corrected by $^{206}Pb/^{238}U$ ages of 15 dated grains is 70.4 ± 0.7 Ma (±1σ); MSWD = 0.60 (Fig. 3b); data scattering is related only to analytical uncertainties.

Thus, the ages of zircon crystallization for two samples (63.0 ± 0.6 and 70.4 ± 0.7 Ma) correspond to the time of syenite emplacement.

Fission-Track Dating of Zircon and Apatite

Fission-track dating is based on counting the fission-track density related to the spontaneous fission of U^{238} nuclei during the geological history [13–15]. The fission-tracks are augmented in size by etching with a special reagent [5, 16], so that they can be counted in minerals under an optical microscope. The accumulation of tracks in minerals with time is a process similar to the accumulation of radiogenic isotopes as a result of radioactive decay. Annealing (disappearance) of fission tracks in most minerals occurs at temperatures of >300°C.

Fission-track annealing depends on time and temperature. As was shown in experiments, the annealing temperature of tracks in apatite is much lower than that in zircon [16]. The annealing process is described in terms of the partial annealing zone (PAZ) as the temperature interval of partial annealing of tracks existing in a mineral. The lower and upper PAZ limits correspond to 10 and 90% of the annealed tracks. PAZ in natural zircon is constrained between 180 and 240°C at heating from 1 to 25 Ma; the respective limits for apatite are 40 and 120°C. The lower PAZ limit determines the temperature of incipient annealing. If it is assumed that the average temperature gradient in the continental crust is 25 °C/km and the average surface temperature is about 10°C, the tracks should be retained in apatite to a depth of ~1.2 km and to 7 km in zircon [17, 18].

The effective closure temperature is another important concept used in fission-track dating. The fission-track system is closed during the cooling of a rock to this temperature within the PAZ, and the fission-track age of the sample marks precisely this moment. It is accepted that more than 50% of fission tracks become stable at the effective temperature of closure [16]. If it is assumed that a sample cools monotonically under conditions typical of geological processes, i.e., at a rate of about 10 °C/Ma, then the effective temperature of closure is 225–240°C for zircon [17] and 105–117°C for apatite [19].

The fission-track age of zircon and apatite was determined at Union College in Schenektady, United States. The minerals were dated using the external track detector method [16]. The zircon grains were pressed into two FEP Teflon^{MT} plates, 2 × 2 cm^2 in size, and apatite grains, into epoxy resin on glass. The laboratory specimens were rough-ground on an abrasive disk and then polished with diamond paste (9 and 1 μm) and alumina paste 0.3 μm during the final stage. Zircon was etched with NaOH–KOH at 228°C for 15 h (first plate) and 25 h (second plate). Apatite was etched by 5M HNO_3 for 20 s at room temperature. The laboratory specimens were covered by a detector (low-U mica) and irradiated in a thermal neutron flux of ~2 × 10^{15} neutron/cm^2 for zircon and 8 × 10^{15} neutron/cm^2 for apatite in the reactor of Oregon University. The age standards and glass-dosimeter with a known U content (CN-5 for zircon and CN-1 for apatite) were irradiated contemporaneously with the samples. The mica was etched with concentrated HF for 15 min at 22°C. The ζ factor [16] for zircon calculated using 12 age standards (Fish Canyon Tuff and Buluk Tuff) is 310.66 ± 6.47 (±1σ). The ζ factor [16] for apatite calculated using 4 age standards (Fish Canyon Tuff and Buluk Tuff) is 112.49 ± 7.53 (±1σ). An Olympus BH-P microscope with automated system and digital data tablet was used for fission-track counting (magn. 1562.5×, dry method). The ZETAAGE 4.7 program designed by M.T. Brandon of Yale University was applied to the calculation of grain ages (Table 2).

The fission-track dating (Table 2) has shown that the last cooling of syenite intrusions below 233 ± 6°C [17] took place 24–25 Ma. According to evidence from the apatite (Table 3), the intrusions cooled below 111 ± 6°C [19] 18–19 Ma ago.

(U–Th)–He Dating

The (U–Th)–He dating is based on the α decay of ^{235}U, ^{238}U, and ^{232}Th with helium as the main daughter product. The ability of the crystalline lattice of solid materials to retain He depends, first of all, on temperature [20]. During the monotonic cooling of apatite with a rate of 10 °C/Ma, He loss from crystals ceases at temperatures below 65 ± 5°C [21], which corresponds to the closure temperature of the (U–Th)–He system. Thus, the (U–Th)–He age marks the timing of rock cooling below 65 ± 5°C.

The (U–Th)–He dating was carried out at Yale University, New Haven, United States. Two aliquots of euhedral apatite grains without inclusions and fractures were dated for each of the samples. Grain size was used for correction of the He loss in compliance with [22]. The (U–Th)–He age of apatite from syenite intrusions was estimated as ~8 Ma. This implies that the syenite cooled below 65°C in the Late Miocene.

Table 2. Fission-track dates of zircon and apatite from syenite intrusions of the Sredinnyi Range, Kamchatka

Sample	Mineral	ρ*s*	*Ns*	ρ*i*	Ni	ρ*d*	*n*	χ^2	Age, Ma	–1σ	+1σ	U ± 2σ	Track length, μm	(*n*)
LA-78	Zircon	5.43	1568	8.82	2547	2.64	20	76.6	25.3	–1.2	+1.3	405.2 ± 29.3		
LA-78	Apatite	0.092	54	0.803	472	28.5	45	29.5	18.4	–2.5	+2.7	11.2 ± 1.2	11.89 ± 1.29	(20)
LA-90	Zircon	10.4	743	16.9	1211	2.62	12	79.6	24.9	–1.4	+1.5	784.7 ± 65.7		
LA-90	Apatite	0.061	59	0.529	511	29.0	36	79.4	18.9	–2.4	+2.7	7.3 ± 0.7	13.06 ± 2.04	(11)
LA-90A	Zircon	10.0	1050	17.0	1779	2.59	20	90.9	23.8	–1.2	+1.3	795.3 ± 61.4		

Note: ρ*s* is the track density of spontaneous ^{238}U fission, $cm^{-2} \times 10^6$; *Ns* is the number of counted tracks of spontaneous fission; ρ*i* is the track density of induced ^{235}U fission, $cm^{-2} \times 10^6$; ρ*d* is the track density in the external detector (low-U mica), $cm^{-2} \times 10^5$; *n* is the number of dated grains; and χ^2 is the ksi-square probability, %.

DISCUSSION

The Emplacement of Syenite Intrusions

According to the U–Pb (SHRIMP) dating, the syenite intrusions in the eastern slope of the Sredinnyi Range of Kamchatka hosted by the metamorphized island-arc sequence of the Andrianovskaya Formation crystallized in the latest Cretaceous or Paleocene (70.4 ± 0.7 and 63.0 ± 0.6 Ma). Four whole-rock samples and three clinopyroxene fractions from the Levoandrianovskii massif yielded an Rb–Sr isochron age of 65.75 ± 0.68 Ma with an initial $^{87}Sr/^{86}Sr$ ratio of 0.703540 ± 0.00006; MSWD = 0.18 [23, 24].

The marginal zones of the syenite intrusions are foliated (M.N. Shapiro, personal communication), which implies that the syenite was, perhaps, emplaced before the metamorphic event superimposed on the Andrianovskaya Formation. The multiphase dunite–clinopyroxenite and clinopyroxene–gabbro massifs, e.g., the Levoandrianovskii massif (Fig. 1), are often regarded as fragments of conduits of Late Cretaceous island-arc complexes (Irunei and Kirganik formations) [25] thrust over the metamorphic rocks of the Andrianovskaya Formation. The deposition of the Irunei Formation of Santonian (?)–Campanian–Maestrichtian age and the Kirganik Formation of Late Campanian (?)–Danian age was related to the evolution of the island arc and the marginal sea separating it from the continental margin [26]. According to the paleomagnetic data, the island arc was situated at a considerable distance south of its present-day location [27]. Thus, the rocks of Irunei, Kirganik, and, probably, the Andrianovskaya formations were localized in the Late Cretaceous and Paleocene south of its modern position, so that the syenite plutons were emplaced into the basement of the island arc that was moving northward.

The collision of the Cretaceous island arc with the Eurasian margin or the Western Kamchatka microplate [28] took place in the Late Paleocene or Early Eocene [29]. The island-arc complexes of the Andrianovskaya Formation and syenite intrusions hosted therein have been obducted onto the continental margin (Kamchatka Group).

Postcollisional Exhumation of Syenite Intrusions

Starting from the Eocene, the syenite intrusions seem to have remained in an authochtonous position, and their further evolution was related to exhumation during growth and erosion of the mountain edifice. The thermochronological data and temperatures of isotopic system closure are summarized in Table 4. According to the fission-track dating of zircon and apatite, the syenite intrusions cooled to temperatures below 233 ± 6°C at approximately 25 Ma and below 111 ± 6°C, at 19 Ma (Fig. 4). If their cooling was monotonic, its rate between 25 and 19 Ma was ~20 °C/Ma. Assuming the geothermal gradient to be 30 °C/km, it can be calculated that the isotherm of 233°C was situated at a depth of about 8 km and 111°C was achieved at a depth of 4 km. This means that the intrusions became closer to the surface by 4 km over 6 Ma (the difference between the fission-track ages of zircon and apatite), and the exhumation velocity was 0.67 km/Ma. Using the fission-track and (U–Th)–He ages of apatite for similar calculations,

Table 3. Results of (U–Th)–He dating of apatite from syenite intrusions of the Sredinnyi Range, Kamchatka

Sample number	Charge number	Corrected age, Ma	Uncertainty (±2σ)
LA-78	1	7.20	0.86
	2	7.98	0.96
LA-90	1	9.04	1.08
	2	8.64	1.03

Table 4. Summary of thermochronological data on syenite intrusions of the Sredinnyi Range, Kamchatka

Geochronological method	Sample	Age, Ma (σ)	Temperature of isotopic system closure, °C
(U–Th)–He (apatite)	LA-78	7.20 ± 0.43	65 ± 5 [21]
		7.98 ± 0.48	
	LA-90	9.04 ± 0.54	
		8.64 ± 0.51	
Fission-track dating (apatite)	LA-78	18.4 ± 2.7	111 ± 6 [19]
	LA-90	18.9 ± 2.7	
Fission-track dating (zircon)	LA-78	25.3 ± 1.3	233 ± 6 [17]
	LA-90	24.9 ± 1.5	
	LA-90A	23.8 ± 1.3	
Rb–Sr isochron for whole-rock samples and clinopyroxene fractions [24]		65.75 ± 0.68	~700 ± 50 [7]
U–Pb, SHRIMP (zircon)	LA-78	63.0 ± 0.6	>900 [8]
	LA-90	70.4 ± 0.7	

the cooling rate between 19 and 8 Ma is estimated at 4 °C/Ma at an exhumation velocity at 0.18 km/Ma. Assuming that the average surface temperature is 10°C, the cooling rate between 8 and 0 Ma is estimated at 7 °C/Ma and the exhumation rate, at 0.25 km/Ma.

The uplift of the Sredinnyi Range of Kamchatka since Oligocene has likely been caused by underplating related to the subduction of the Pacific plate beneath Kamchatka. The underplating rate seems to have been close to the exhumation rate, estimated at 0.18–0.67 km/Ma.

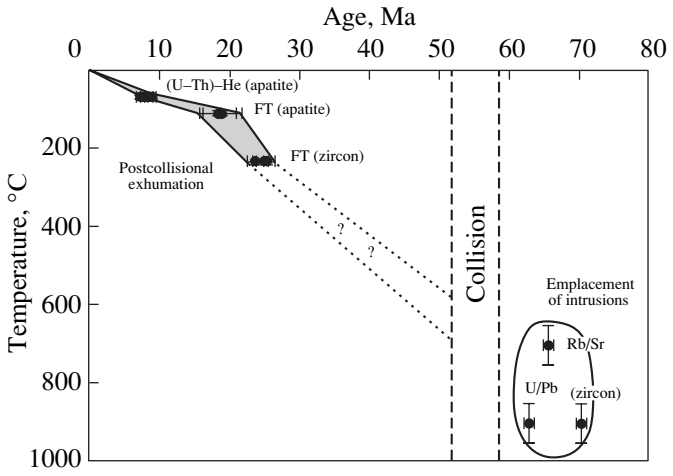

Fig. 4. Thermochronological and tectonic history of syenite intrusions on the eastern slope of the Sredinnyi Range of Kamchatka. The age of Cretaceous island arc collision in central Kamchatka is given after [29]. The summary data are presented in Table 4; FT is the fission-track age.

CONCLUSIONS

(1) The syenite intrusions in the eastern slope of the Sredinnyi Range of Kamchatka considered in this paper demonstrate that the velocity of rock exhumation can be evaluated on the basis of thermochronological data.

(2) According to the U–Pb (SHRIMP) dating of zircon, the syenite intrusions were emplaced in the Late Cretaceous or Early Paleogene (63.0 ± 0.6 Ma or 70.4 ± 0.7 Ma).

(3) Starting from 25 Ma, the rate of intrusion cooling due to exhumation varied from 4 to 20 °C/Ma.

(4) If the geothermal gradient was 30 °C/km, the exhumation velocity over the past 25 Ma ranged from 0.18 to 0.67 km/Ma.

ACKNOWLEDGMENTS

We thank N.A. Bogdanov, M.N. Shapiro, and G.E. Bondarenko for fruitful discussions on the subject of this paper. The study was supported by the Russian Foundation for Basic Research, project nos. 01-05-64019, 02-05-64967, and the National Science Foundation (USA), grant no. OPP-9911910.

REFERENCES

1. A. V. Rikhter, Geotektonika **28** (1), 71 (1995).
2. G. B. Flerov and A. V. Koloskov, *Alkaline Basaltic Magmatism in Central Kamchatka* (Nauka, Moscow, 1976) [in Russian].
3. J. K. Hourigan, M. T. Brandon, J. I. Garver, and A. V. Solov'ev, in *Proceedings 7th Zonenshain International Conference on Plate Tectonics* (Nauchnyi Mir, Moscow, 2001), p. 504.

4. *Interpretation of Geochemical Data*, Ed. by E. V. Sklyarov (Intermet Inzhiniring, Moscow, 2001) [in Russian].
5. G. Faure, *Principles of Isotope Geology* (Wiley, New York, 1986; Mir, Moscow, 1989).
6. M. H. Dodson, Contrib. Mineral. Petrol. **40,** 259 (1973).
7. W. B. Harland, R. L. Armstrong, and A. V. Cox, *A Geologic Time Scale* (Cambridge Univ. Press, Cambridge, 1990).
8. J. K. W. Lee, I. S. Williams, and D. J. Ellis, Nature **390** (6656), 159 (1997).
9. J. B. Paces and J. D. Miller, J. Geophys. Res. **98,** 13 997 (1993).
10. R. J. Muir, T. R. Ireland, S. D. Weaver, and J. D. Bradshaw, Chem. Geol. **127** (1–3), 191 (1996).
11. I. S. Williams, Rev. Econ. Geol. **7,** 1 (1998).
12. G. L. Cumming and J. R. Richards, Earth Planet. Sci. Lett. **28** (2), 155 (1975).
13. P. B. Price and R. M. Walker, J. Geophys. Res. **68,** 4847 (1963).
14. R. L. Fleischer, P. B. Price, and R. M. Walker, *Nuclear Tracks in Solids: Principles and Applications* (Univ. California Press, Berkeley, 1975).
15. Yu. A. Shukolyukov, I. N. Krylov, I. N. Tolstikhin, and G. V. Ovchinnikova, Geokhimiya, No. 3, 291 (1965).
16. G. A. Wagner and P. Van Den Haute, *Fission-Track Dating* (Kluwer Academic, Dordrecht, 1992).
17. M. T. Brandon and J. A. Vance, Am. J. Sci. **292,** 565 (1992).
18. M. T. Brandon, M. K. Roden-Tice, and J. I. Garver, Geol. Soc. Am. Bull. **110** (8), 985 (1998).
19. G. M. Laslett, P. F. Green, I. R. Duddy, and A. J. W. Gleadow, Chem. Geol. **65** (1), 1 (1987).
20. P. W. Reiners, Eos **83,** 21 (2002).
21. K. A. Farley, J. Geophys. Res. **105** (2), 2903 (2000).
22. K. A. Farley, R. A. Wolf, and L. T. Silver, Geochim. Cosmochim. Acta **60** (21), 4223 (1996).
23. E. A. Landa, B. A. Markovskii, E. G. Sidorov, and B. I. Slyadnev, in *The Petrology and Metallogeny of Basic–Ultrabasic Rock Complexes in the Kamchatka Region* (Nauchnyi Mir, Moscow, 2001), pp. 87–105 [in Russian].
24. B. V. Belyatskii, E. A. Landa, B. A. Markovskii, and E. G. Sidorov, Dokl. Akad. Nauk **382** (2), 235 (2002) [Dokl. Acad. Sci. **382** (2), 49 (2002)].
25. G. B. Flerov, P. I. Fedorov, and T. G. Churikova, Petrologiya **9** (2), 189 (2001) [Petrology **9** (2), 161 (2001)].
26. V. P. Zinkevich, S. Yu. Kolodyazhnyi, L. G. Bragina, *et al.*, Geotektonika **28** (1), 81 (1994).
27. D. V. Kovalenko, E. V. Shiryaevskii, V. L. Zlobin, and A. V. Nosorev, Fiz. Zemli, No. 6, 1 (2000).
28. N. A. Bogdanov and V. D. Chekhovich, Geotektonika, No. 1, 72 (2002) [Geotectonics, No. 1, 63 (2002)].
29. E. A. Konstantinovskaya, Tectonophysics **325** (1/2), 87 (2000).